Mice hypomorphic for Pitx3 show robust entrainment of circadian behavioral and metabolic rhythms to scheduled feeding

Scarpa, L.L.; Wanken, B.; Smidt, M.; Mistlberger, R.E.; Steele, A.D.

DOI
10.1016/j.celrep.2021.109865

Publication date
2022

Document Version
Final published version

Published in
Cell Reports

Cell Reports

CellPress
OPEN ACCESS

Matters Arising

Mice hypomorphic for *Pitx3* show robust entrainment of circadian behavioral and metabolic rhythms to scheduled feeding

Lori L. Scarpa,[1] Brad Wanken,[2] Marten Smidt,[3] Ralph E. Mistlberger,[4,*] and Andrew D. Steele[1,5,*]
[1]Department of Biological Sciences, California State Polytechnic University Pomona, Pomona, CA 91768, USA
[2]Rodent Metabolic Core, Saban Research Institute, Children's Hospital Los Angeles, Los Angeles, CA 90027, USA
[3]Swammerdam Institute for Life Sciences, University of Amsterdam, Amsterdam 94246, the Netherlands
[4]Department of Psychology, Simon Fraser University, Burnaby, BC V5A 1S6, Canada
[5]Lead contact
*Correspondence: mistlber@sfu.ca (R.E.M.), adsteele@cpp.edu (A.D.S.)
https://doi.org/10.1016/j.celrep.2021.109865

SUMMARY

Pitx3^{ak} mice lack a functioning retina and develop fewer than 10% of dopamine neurons in the substantia nigra. Del Río-Martín et al. (2019) reported that entrainment of circadian rhythms to daily light-dark (LD) cycles is absent in these mice, and that rhythms of locomotor activity, energy expenditure, and other metabolic variables are disrupted with food available *ad libitum* and fail to entrain to a daily feeding. The authors propose that retinal innervation of the suprachiasmatic nucleus is required for development of cyclic metabolic homeostasis, but methodological issues limit interpretation of the results. Using standardized feeding schedules and procedures for distinguishing free-running from entrained circadian rhythms, we confirm that behavioral and metabolic rhythms in Pitx3^{ak} mice do not entrain to LD cycles, but we find no impairment in circadian organization of metabolism with food available *ad libitum* and no impairment in entrainment of metabolic or behavioral rhythms by daily feeding schedules. This Matters Arising paper is in response to Del Río-Martín et al. (2019), published in *Cell Reports*. See also the response by Fernandez-Perez et al. (2022), published in this issue.

INTRODUCTION

Circadian rhythms in mammals are controlled by a master, light-dark (LD) entrainable pacemaker in the hypothalamic suprachiasmatic nucleus (SCN) and food-entrainable circadian oscillators in many other brain regions and most body tissues (Damiola et al., 2000; Dibner et al., 2010; Golombek and Rosenstein, 2010). Entrainment to LD cycles is mediated by intrinsically photoreceptive retinal ganglion cells that project to the SCN (Foster et al., 2020). Entrainment of circadian metabolic rhythms to feeding cycles is likely mediated by multiple feeding-related signals that may be universal or tissue specific (Mistlberger, 2020; Schibler, 2009). Entrainment of behavioral (food-anticipatory) rhythms to feeding schedules likely also involves multiple signals, among which a dopamine projection from the substantia nigra (SN) to circadian oscillators in the dorsal striatum may play an important role (Gallardo et al., 2014a; Hood et al., 2010; Mistlberger, 2020).

Del Río-Martín et al. (2019) recently reported in *Cell Reports* that mice harboring a homozygous hypomorphic mutation in the promoter region of *paired-like homeodomain 3* (*Pitx3*) exhibit a marked impairment in both LD and food entrainment. *Pitx3^{ak}* mutant mice were found to free-run in the presence of LD when food was available *ad libitum*, and showed disrupted rhythms of metabolism; plasma corticosterone; clock gene expression in the SCN, liver, and brown adipose tissue; and food intake control genes in the arcuate nucleus and ventromedial hypothalamus. When food was restricted to the 12-h dark period, *Pitx3^{ak}* mutant mice failed to show synchrony of energy expenditure (EE), locomotor activity, and plasma corticosterone to feeding time, and no rhythm of food-anticipatory activity emerged. The authors concluded that lack of light input disrupts SCN development and thereby irreversibly impairs cyclic metabolic homeostasis.

Pitx3 plays a key role in determination of cell fate in development (Lamonerie et al., 1996) and is responsible for activating expression of the *tyrosine hydroxylase* gene, which is required for synthesis of dopamine (Lebel et al., 2001). *Pitx3^{ak}* mutant mice lack a lens, fail to develop a functional retina, and are blind (Del Río-Martín et al., 2019). In the brain, expression of *Pitx3* is essential for the development of dopamine neurons in the SN (Nunes et al., 2003; Smidt and Burbach, 2007), and *Pitx3^{ak}* mice exhibit a >90% reduction in dopamine innervation specific to the dorsal striatum (Hwang et al., 2005). The findings of Del Río-Martín et al. (2019) that *Pitx3^{ak}* mice do not entrain to either LD or feeding schedules are therefore consistent with the known role of the retina in circadian photoentrainment and with the proposed role for dorsal striatal dopamine innervation in food entrainment.

The retinal defects and absence of photic entrainment in *Pitx3*^{ak} mice were clearly demonstrated by Del Río-Martín et al. (2019), but the methods used to assess entrainment of metabolism and behavior by daily feeding schedules raise interpretative issues. Most, if not all, of the reported impairments in circadian organization of metabolism and entrainment to feeding schedules appear to be artifacts of averaging data from blind *Pitx3*^{ak} mice without controlling for differences in the circadian phase of the free-running SCN pacemaker. Also, food entrained rhythms of activity and corticosterone are unlikely to emerge when food is available for 12 h/day without caloric restriction (Honma et al., 1983). Here, using the same *Pitx3*^{ak} mutant mouse strain, we confirm the absence of photic entrainment and the marked reduction in the number of SN dopamine neurons but do not observe impaired circadian organization of activity or metabolism with food available *ad libitum*, and we see no impairment of entrainment to restricted feeding schedules. The *Pitx3*^{ak} mutant mouse model therefore does not provide support for a proposal that retinal innervation of the SCN is required for normal development of cyclic metabolic homeostasis or food entrainment in mice.

RESULTS

Pitx3^{ak} mice fed *ad libitum* in LD exhibit free-running but otherwise normal circadian metabolic rhythms

To phenotype behavioral and metabolic circadian rhythms in *Pitx3*^{ak} mice, we conducted two experiments using separate cohorts of mutant and control mice. In experiment 1, young adult *Pitx3*^{ak} and control mice (six male and six females per group) were housed individually in metabolic cages (TSE LabMaster/PhenoMaster) to measure food intake, locomotor activity, O_2 consumption (VO_2), CO_2 production (VCO_2), EE, and respiratory exchange ratio (RER) (indirect calorimetry).

Data on body weight, body composition, daily activity, and EE levels, for males and females, are provided in Figure S1. Compared with control mice, *Pitx3*^{ak} mice had lower body mass, fat mass, and lean mass. *Pitx3*^{ak} mice also ate less, although not when normalized to body weight, and showed a trend for more activity. In both the *Pitx3*^{ak} and control groups, males were heavier and had more fat mass than females, while females showed higher EE. There were no sex differences in lean mass, food intake per gram body weight, and total daily activity (Figure S1).

With food available *ad libitum* for 3 days in the metabolic chambers, control mice were active and ate predominantly at night, and exhibited daily rhythms of EE and RER with a nocturnal peak (Figures 1A and 1B). Individual *Pitx3*^{ak} mice also exhibited circadian variations in metabolic variables, but the rhythms were not synchronized with the LD cycle or with other mice (Figures 1C and 1D). To compare metabolic rhythms between groups, we aligned EE and RER waveforms from individual *Pitx3*^{ak} mice by the first peak in the time series (Figures 1E and 1F) and then averaged across mice (n = 12, pooled by sex). The *Pitx3*^{ak} group average waveforms were then aligned with group average waveforms from the control mice (n = 12; Figures 1G and 1H). These overlays clearly show that circadian variations of EE and RER in *Pitx3*^{ak} mice are essentially indistinguishable from control mice, despite the lack of entrainment to LD. Circadian variations of VO_2 and VCO_2 closely paralleled EE, as expected. The only significant difference between groups was that EE, VO_2, and VCO_2 were higher throughout the circadian cycle in the *Pitx3*^{ak} mice (see Figures S1 and S2 for non-normalized EE). Elevated EE in the *Pitx3*^{ak} mice presumably reflects the significantly lower body mass and somewhat elevated activity levels.

Metabolic activity and locomotor activity varied in synchrony in all *Pitx3*^{ak} and control mice. The tight coupling between metabolism and locomotion is clearly evident in running waveforms of EE and activity counts in 10-min time bins for representative mice in each group (Figures 1I–1L). Correlations between EE and locomotor activity in individual mice, across the 3 days of *ad libitum* food access (432 time bins) were strongly positive and slightly higher in the *Pitx3*^{ak} group (controls = +0.61 ± 0.09; *Pitx3*^{ak} = +0.71 ± 0.09; unpaired t_{10} = 2.923; p = 0.015; Figure 1M).

Circadian metabolic rhythms in *Pitx3*^{ak} synchronize to daily feeding schedules

Del Río-Martín et al. (2019) reported that *Pitx3*^{ak} mice fed only during the 12-h dark period failed to synchronize metabolic rhythms with the 24-h feeding schedule. To evaluate entrainment of metabolism to daily feeding schedules, *Pitx3*^{ak} and control mice in experiment 1 were restricted to 80% of group mean *ad libitum* caloric intake, provided each day 6 h before lights-off, for 28 days. The mice were continuously monitored in the metabolic cages on days 1–4 and 26–28 of food restriction.

Group mean and individual waveforms of hourly (Figure 2A; Figures S3A–S3F), 10-min (Figures 3A–3D), and cumulative food intake (Figures S3G and S3H) indicate that *Pitx3*^{ak} and control mice consumed 85%–95% of the daily food allotment within ~12 h, with a range of 8–22h for individual mice across days, and no group differences. All the mice began eating immediately at food delivery, with secondary peaks of food intake evident in most mice 5–6 h later. By day 28 of food restriction, body weight in male mice was reduced by 7.0% ± 1.3% in the *Pitx3*^{ak} group and 4.2% ± 1.6% in the control group (between groups, t_{10} = 4.05, p = 0.0023; Figure S3I). Weight loss in female mice was more variable and not significant in group data for *Pitx3*^{ak} (0.2% ± 4.8%) or the control (1.8% ± 2.2%) groups (Figure S3J).

Circadian variations of RER, VO_2, VCO_2, and EE synchronized to the daily feeding schedule in all mice (Figures 2C–2F). The effect is particularly striking in the average waveforms for the *Pitx3*^{ak} male and female groups, which showed no group rhythm when food was available *ad libitum*, but rapid emergence of group synchrony when food was restricted. In the control mice, the nocturnal peaks in the metabolic rhythms were phase advanced (Figures 2C–2F). To compare groups, cosine functions were fit to the RER rhythms for each mouse, and rhythm acrophases were averaged across the 3 days of *ad libitum* food access and days 1–2, 3–4, and 26–28 of restricted feeding (Figures 3E–3H). Repeated-measures ANOVA confirmed a significant main effect of restricted feeding ($F_{1,20}$ = 8.804, p = 0.0076), but no main effect of group ($F_{3,20}$ = 2.157, p = 0.125). Post hoc tests confirmed a significant phase advance of RER acrophase in the control groups (p < 0.001), but no difference in acrophase between control and *Pitx3*^{ak} groups during restricted feeding.

CellPress
OPEN ACCESS

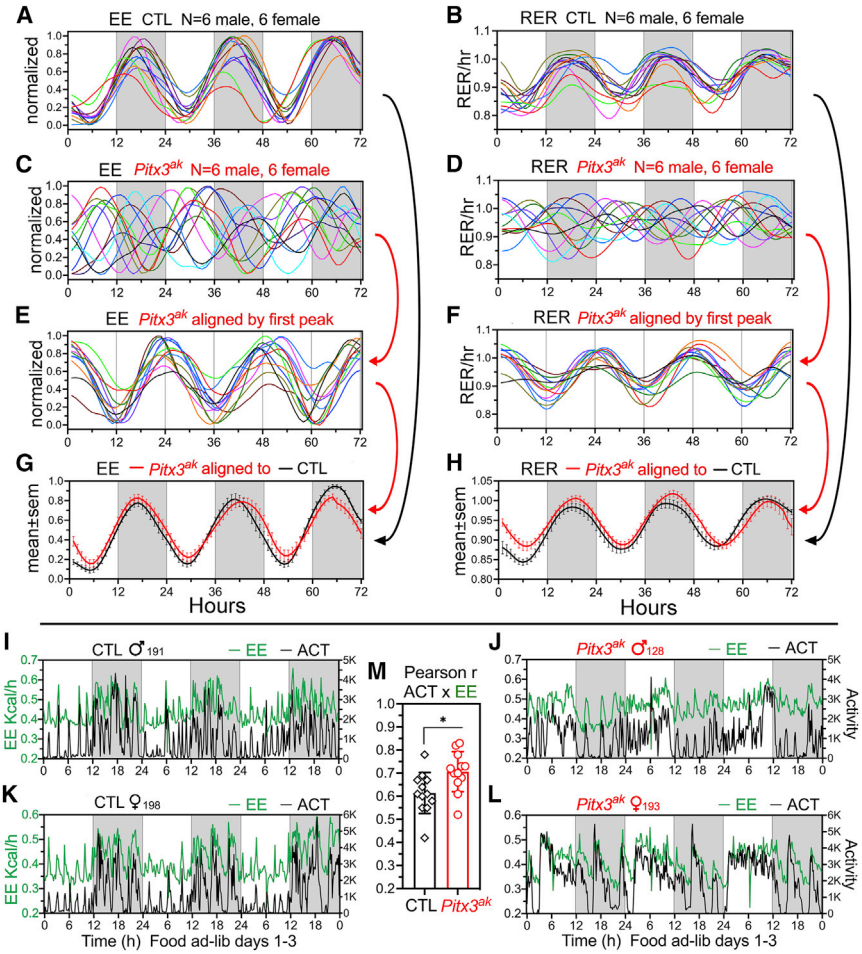

Figure 1. Circadian metabolic rhythms free-run but are robust in *Pitx3*^{ak} mice fed *ad libitum*

(A and B) Smoothed running waveforms of energy expenditure (EE; normalized) and respiratory exchange ratio (RER; not normalized) from six male and six female control mice (individuals coded by color).

(C and D) EE and RER from *Pitx3*^{ak} mice showing lack of synchrony of individuals when food is available *ad libitum*.

(E and F) EE and RER from *Pitx3*^{ak} mice after aligning the waveforms to the first peak.

(G and H) Group average (±SEM) EE and RER, with *Pitx3*^{ak} mice (red curve) aligned to the control mice (black curve).

(I–L) EE (green curves) and locomotor activity (black curves) of representative *Pitx3*^{ak} and control male and female mice, illustrating synchrony between activity and metabolism.

(M). Correlation coefficients quantifying the association between activity and EE in individual control and *Pitx3*^{ak} mice (unpaired t test, $p < 0.05$). Gray shading denotes lights off.

The circadian rhythms of VO_2, VCO_2, and EE were also shifted in parallel by the restricted daytime feeding schedule (Figures 2D–2F). Differences between the *Pitx3*^{ak} and control groups primarily reflect the greater amount of activity expressed prior to mealtime in the *Pitx3*^{ak} mice and the increased EE evident throughout the day, as was observed when food was available *ad libitum* prior to restricted feeding. These results indicate no failure of metabolic rhythms to synchronize to daily feeding schedules in *Pitx3*^{ak} mice.

Circadian metabolic and activity rhythms are synchronized in food-restricted *Pitx3*^{ak} mice

Del Río-Martín et al. (2019) also reported that *Pitx3*^{ak} mice fail to anticipate scheduled feeding. Group mean waveforms of activity during restricted feeding in our mice reveal increased activity prior to mealtime on days 26–28 of caloric restriction in the *Pitx3*^{ak} male and female groups and in the control female group (Figure 2B). Waveforms from individual mice show activity beginning to rise ~3 h prior to mealtime and increasing to a peak at mealtime (e.g., Figures 3I–3L). This food-anticipatory activity pattern was weak or absent in some mice, including all of the male control mice (e.g., Figures 2B and 3I).

For group comparisons, anticipatory activity was quantified as a ratio of activity during the 3 h prior to mealtime relative to total daily activity. Anticipation ratios were averaged over the last 3 days of restricted feeding (R26–28) and compared with ratios calculated for the 3 days of *ad libitum* food access. Two-way repeated-measures ANOVA confirmed a significant main effect of restricted feeding ($F_{1,20}$ = 32.29, $p < 0.0001$) and group ($F_{3,20}$ = 9.859, $p = 0.0003$) and a significant interaction ($F_{3,20}$ = 3.226, $p = 0.044$). Post hoc tests (Sidak's) comparing food restriction with *ad libitum* days indicate significant anticipation in the male and female *Pitx3*^{ak} groups and in the female control group (Figures 3M and 3O). Low food anticipation ratios in male control mice likely reflect the prolonged duration of eating, the prominent second peak of feeding at dark onset in this group (6 h after the first peak of feeding), and modest weight loss.

Visual inspection of group mean (Figure 2) and individual (Figures 3I–3L) waveforms clearly reveals a high degree of synchrony between metabolic rhythms and locomotor activity in all groups. Correlations between the amount of food-anticipatory activity and EE were strongly positive in all groups, with higher correlation coefficients again evident in the *Pitx3*^{ak} mice (Figures 3N and 3P). These analyses provide no evidence that the *Pitx3*^{ak} mutation impairs the ability of mice to anticipate a daily mealtime or disrupts synchrony between locomotor activity and metabolic rhythms during food restriction.

Food-anticipatory activity rhythms are robust in free-running *Pitx3*^{ak} mice

In experiment 1, caloric restriction was set at 80% of *ad libitum* in control and *Pitx3*^{ak} mice, weight loss was mild or absent, and

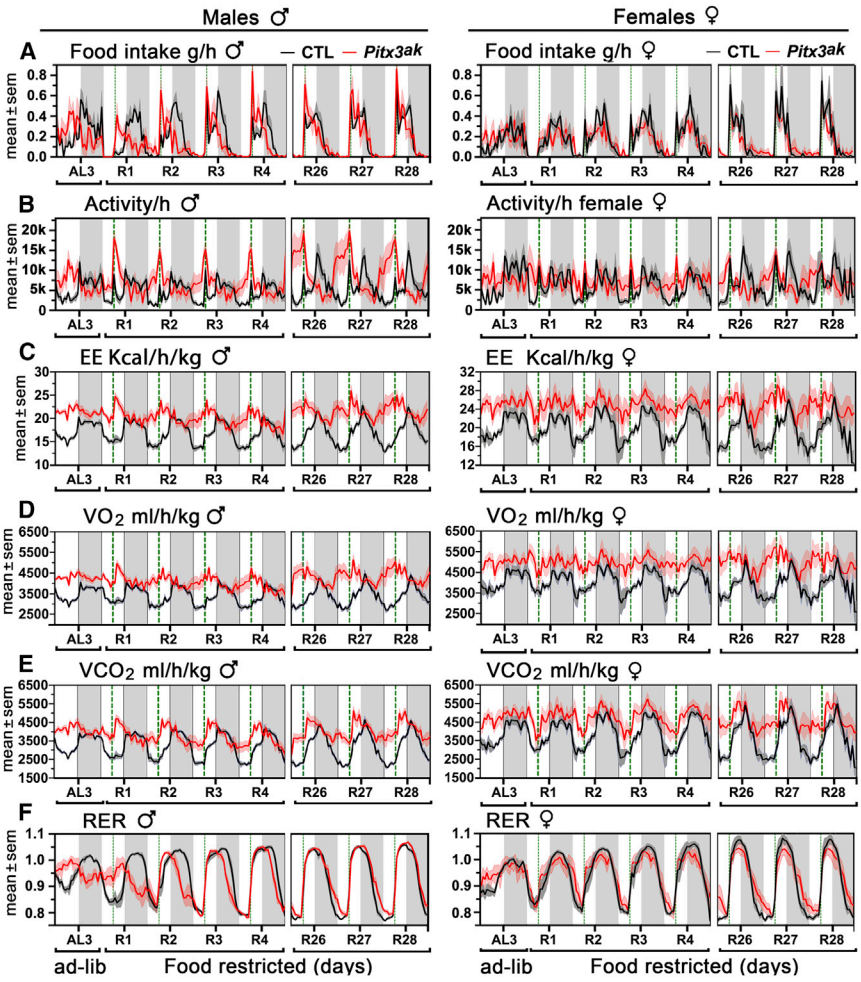

Figure 2. Circadian rhythms of activity and metabolism synchronize to a daily feeding schedule in control and *Pitx3*^{ak} mice

Data are group mean (±SEM) hourly averages across the last day of food *ad libitum* (AL3) and the first 4 days (R1–4) and the last 3 days (R26–28) of restricted feeding (80% of *ad libitum* caloric intake provided daily 6 h after lights on).

(A–F) Food intake (grams) (A), locomotor activity (where k denotes thousand) (B), RER (C), oxygen consumption (VO_2) (D), carbon dioxide production (CO_2) (E), and EE (F). Gray shading denotes lights off. Control (CTL) groups are coded black and *Pitx3*^{ak} groups are coded red. Male groups are in the left column and female groups in the right column (n = 6 per group).

food anticipation was weak in many cases, particularly in male controls. In experiment 2, the level of caloric restriction was adjusted to promote expression of food-entrained anticipatory activity, and mice were recorded continuously for up to 55 days of restricted feeding, to further assess food-anticipatory rhythms and determine whether anticipation in the blind *Pitx3*^{ak} mice is independent of free-running rhythms or involves entrainment of free-running rhythms.

Young, female, age-matched *Pitx3*^{ak} (n = 7) and control mice (n = 8) were housed individually in cages equipped with photobeams. With food available *ad libitum*, locomotor activity was 78% ± 6% nocturnal in control mice, but free-ran with a periodicity in the 23.25–23.83 h range in *Pitx3*^{ak} mice (mean ± SD, 23.56 ± 0.24 h; Figures 4B1–4H1 and S4). Apart from the failure to entrain to LD, locomotor activity rhythms in the *Pitx3*^{ak} and control mice were remarkably similar (see Figure S3 for group comparisons of activity rhythm parameters with food available *ad libitum*).

In our previous work with adult C57BL/6J mice, a 60% caloric restriction schedule resulted in weight loss in the 10%–20% range and reliably induced a robust circadian rhythm of food-anticipatory activity (Gallardo et al., 2014b). In preliminary work with *Pitx3*^{ak} mice, 60% caloric restriction led to excessive weight loss. Caloric restriction adjusted to 80% for the *Pitx3*^{ak} mice and maintained at 60% for control mice resulted in equivalent weight loss in the two groups (8.4% ± 3.6% and 16.9% ± 2.5%, respectively; $p > 0.05$).

Under this feeding regimen, all control mice exhibited robust food-anticipatory activity within the first week of restricted feeding (e.g., Figure 4A1). Activity began to rise ~3 h prior to mealtime and increased monotonically to a peak at expected mealtime (e.g., Figures 4A2 and 4A3). Nocturnal activity decreased but remained synchronized to the LD cycle. Total daily (24 h) activity during restricted feeding decreased by 25.7% ± 6.6% (Figure 4K; paired $t_7 = 4.797$, $p = 0.002$)

Del Río-Martín et al. (2019) reported that clock gene rhythms in the SCN of *Pitx3*^{ak} mice were absent with food available *ad libitum*, but rescued by 12 h/day restricted feeding, implying that free-running rhythms in these mice were entrained to the feeding schedule. Free-running activity rhythms in our *Pitx3*^{ak} mice show no evidence of entraining to the daily feeding schedule, but a bout of activity anticipating mealtime was clearly visible in the actograms when mealtime occurred during the rest phase of the free-running rhythm (Figures 4B1–4H1). Activity profiles generated by averaging across a week of these days for each mouse confirmed significant food anticipation beginning 2–3 h prior to mealtime and rising to a peak at mealtime (Figures 4B2–4F2). Averaging across all days of restricted feeding completely or substantially removed the contribution of the free-running activity rhythm to the activity profiles, and highlighted mealtime as the determinant of a 24-h rhythm of food-anticipatory activity in these mice (Figures 4B3–4F3).

Overlays of normalized group mean activity waveforms from the *Pitx3*^{ak} and control mice further highlight the similar timing and duration of food anticipation in the two groups (Figures 4I and 4J). Compared with control mice, *Pitx3*^{ak} mice showed significantly more activity counts during the 3 h prior to mealtime

CellPress
OPEN ACCESS

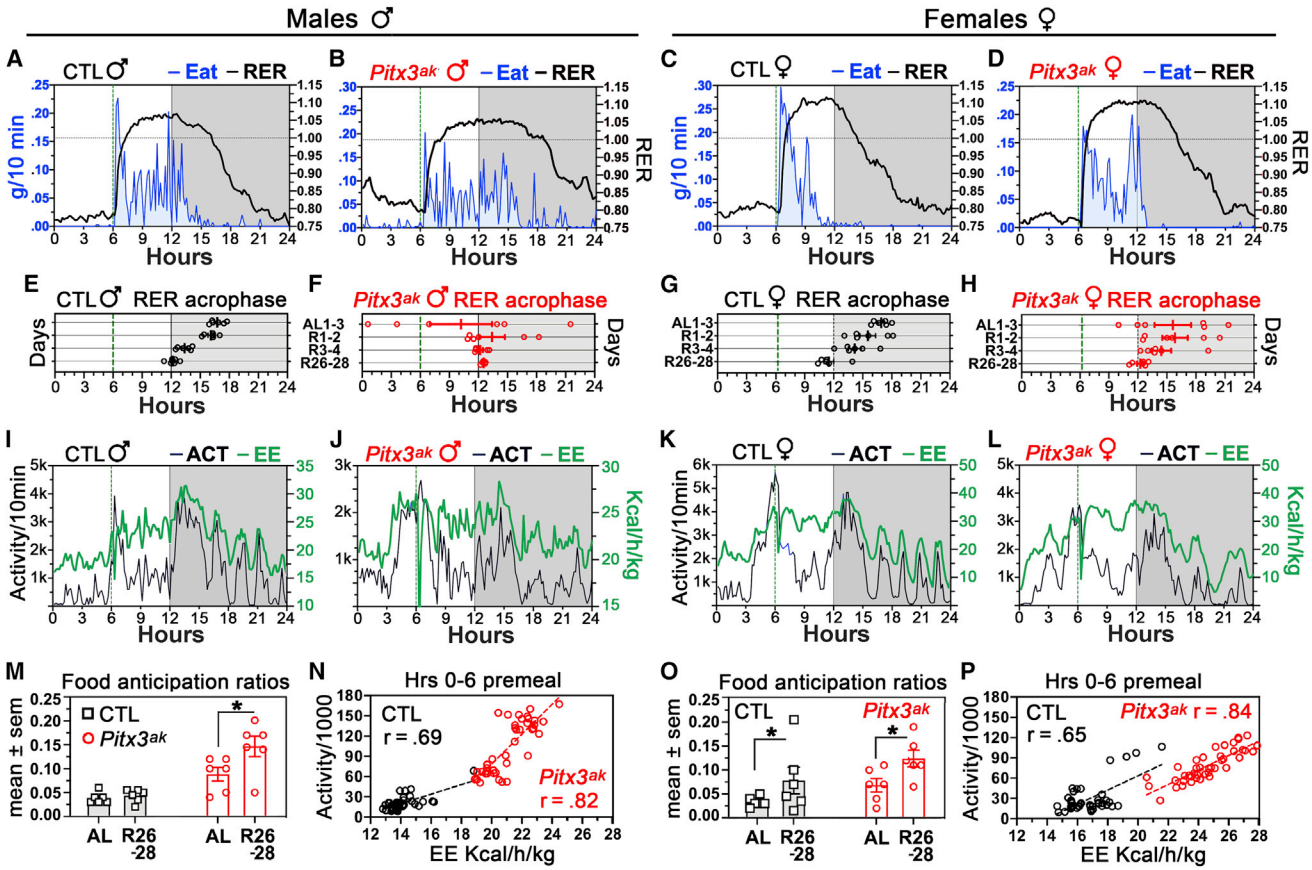

Figure 3. Circadian rhythms of activity and metabolism synchronize to a daily feeding schedule in *Pitx3*^{ak} mice

(A–D) Food intake (blue line and shading) and RER per 10-min time bin averaged over the last 3 days of restricted feeding in representative male and female control and *Pitx3*^{ak} mice.

(E–H) Acrophase of the daily rhythm of RER for individual mice averaged over *ad libitum* food access days (AL) 1–3 and restricted feeding days R1–2, R3–4, and R26–28.

(I–L) Locomotor activity (ACT) and EE per 10-min time bin averaged over the last 3 days of restricted feeding in the same representative mice.

(M and O) Food anticipation ratios averaged over the last 3 days of restricted feeding (R26-28) and the last 3 days of *ad libitum* food access (AL) for statistical comparison. *p < 0.05 (Sidak's post hoc test).

(N and P) Correlation between activity and EE during the 6 h prior to mealtime on the last 3 days of restricted feeding (Pearson correlation coefficient r; n = 6 per group).

(t_{13} = 3.282, p = 0.006; Figure 4L), but there was no group difference when anticipatory activity was expressed as a ratio relative to total daily activity (t_{13} = 0.876, p = 0.3967; Figure 4M). Unlike control mice, the *Pitx3*^{ak} mice did not show a significant reduction in total daily activity during restricted feeding (t_6 = 0.31, p = 0.76), and activity levels remained higher than in controls (t_{13} = 3.89, p = 0.0019; Figure 4K), as it was prior to restricted feeding.

Tyrosine hydroxylase (TH)-expressing neurons in the SN are markedly reduced in *Pitx3*^{ak} mice

To confirm that our *Pitx3*^{ak} mice expressed the known effect of this mutation on the development of dopamine neurons in the SN, we harvested, sectioned, and immunolabeled brains for TH (Figure S5). As expected, in sagittal sections, control mice showed dense labeling of TH-positive fibers in the striatum, nucleus accumbens, and olfactory tubercle (Figure S5A). In contrast, there was substantially less innervation of the striatum and nucleus accumbens in the *Pitx3*^{ak} sections, whereas the olfactory tubercle appeared strongly stained (Figure S5B). Control midbrains showed numerous dopamine neurons in the VTA and SN (Figure S5C), while the *Pitx3*^{ak} midbrain showed very little TH staining in the SN but ample staining in the VTA (Figure S5D).

DISCUSSION

Del Río-Martín et al. (2019) reported that mice bearing the *Pitx3*^{ak} mutation free-run in the presence of 24-h LD cycles exhibit disrupted metabolic rhythms when food is available *ad libitum*, and they fail to entrain locomotor activity and metabolic rhythms to a daily feeding schedule. Our results confirm the absence of LD entrainment in *Pitx3*^{ak} mice but reveal otherwise normal circadian organization of activity and metabolism with food available

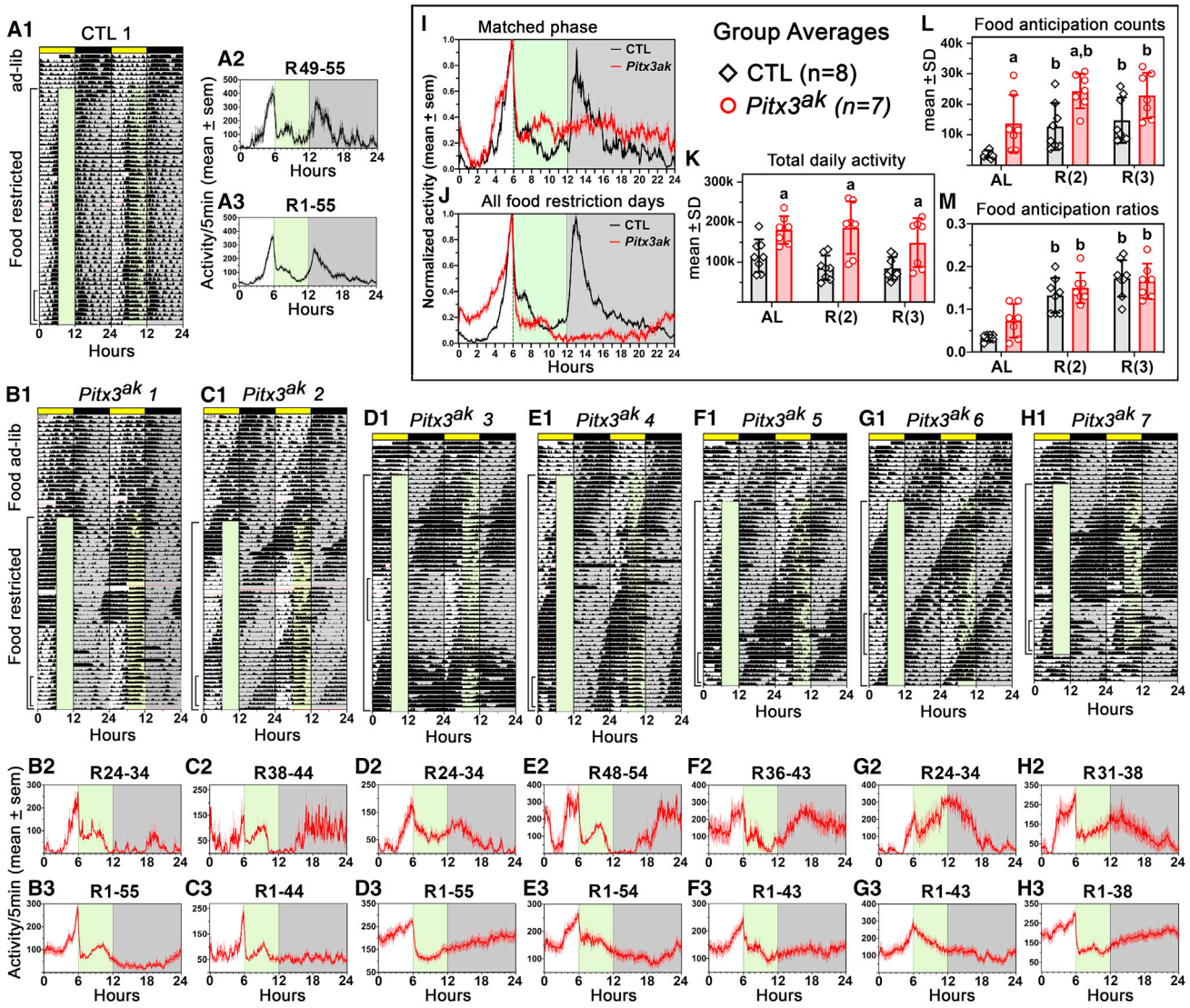

Figure 4. Circadian anticipatory activity rhythms entrain to scheduled feeding in *Pitx3*^{ak} mice

(A1) Double-plotted actogram of locomotor activity in 10-min time bins from a representative control mouse with food available *ad libitum* and then restricted to 60% of free-feeding caloric intake, provided 6 h after lights on each day for 55 days. Green shading denotes the first 6 h of feeding, during which most of the food was eaten, but feeding was not time limited. (A2) Average waveform for days 49–55 of restricted feeding in this mouse. (A3) Average waveform for days 1–55 of restricted feeding for this mouse.

(B1–H1) Actograms for all days of recording in the seven *Pitx3*^{ak} mice. (B2–H2) Activity waveforms for 6–10 days when the free-running rhythm did not overlap with the hours before mealtime. The shorter of the two brackets to the left of each actogram indicates which set of days was used for the averaging. (B3–H3) Activity waveforms for all days of food restriction.

(I) Group mean waveforms created by normalizing individual waveforms from *Pitx3*^{ak} mice (n = 7) in (B2)–(H2) (red curve) and in all control mice (n = 8) (A2 and seven others not shown), and then normalizing the group mean waveforms to emphasis the common shape of the waveforms in the two groups.

(J) The same as (I), but using data from (A3) and (B3)–(H3).

(K) Group mean (±SD) total daily activity in control (black) and *Pitx3*^{ak} (red) mice during *ad libitum* food access (AL) and during the sets of restricted feeding days represented in (A2)–(H2) (labeled R(2)) and (A3)–(H3) (labeled R(3)).

(L) Activity during the 3 h prior to meal onset.

(M) Ratios of activity during the 3 h prior to meal onset relative to total daily activity. In the bar graphs, "a" denotes significant ($^{a}p < 0.05$) differences between groups, and "b" denotes significant differences between restricted feeding days and *ad libitum* food access days within groups.

ad libitum and no impairment of entrainment to feeding schedules.

Pitx3^{ak} mice cannot entrain to LD cycles, and with food available *ad libitum*, they free-run with a circadian period that varies across individuals. Averaging data from free-running animals, as was done by Del Río-Martín et al. (2019), without controlling for differences in circadian phase will most likely yield group mean waveforms that approach a flat line, such as those

presented by Del Río-Martín et al. (2019) for locomotor activity, food intake, EE, plasma corticosterone, expression of clock genes in the SCN, VMH, liver, and BAT, and expression of food intake regulatory genes in the arcuate nucleus, in *Pitx3*^{ak} mice fed *ad libitum*. When free-running activity and metabolic rhythms in groups of *Pitx3*^{ak} mice fed *ad libitum* are aligned to a common phase (e.g., locomotor activity onset or the peak of the metabolism rhythm, respectively), we find circadian organization to be as robust as in control mice. The similarity between *Pitx3*^{ak} and control mice is all the more striking given that the control mice were entrained to the LD cycle, and entrained rhythms typically have a higher amplitude than free-running rhythms.

When food was restricted to the 12-h dark period, Del Río-Martín et al. (2019) reported that this "is not sufficient to synchronize cyclic energy metabolism in Pitx3^{ak} mice and their locomotor activity is not altered by restrictions of the availability of food." The lack of synchrony of metabolism and activity to the feeding schedule may be because of lack of caloric restriction, because total daily food intake in their mice was reported to increase during the feeding schedule compared with *ad libitum* access. The Pitx3^{ak} mice were lighter than the control mice after restricted feeding, but weight change within groups was not reported. In experiment 1, we restricted caloric intake to 80% of *ad libitum*, and although some of the mice did not lose weight, metabolic rhythms synchronized to mealtime in all mice and were clearly evident in Pitx3^{ak} group data without the need for alignment. Differences between Pitx3^{ak} and control mice in the waveform of the EE rhythms reflected elevated EE across the day and more activity prior to mealtime in the Pitx3^{ak} mice.

Del Río-Martín et al. (2019) interpreted the absence of food-anticipatory activity in *Pitx3*^{ak} mice as evidence of a defect in food entrainment, but this is likely due to the lack of caloric restriction and the extended duration of daily food access (12 h/day). Previous studies have shown that food anticipation is weak or absent when food is provided for 12 h without caloric restriction (e.g., LeSauter et al., 2020; Stephan and Becker, 1989), so we would not expect to see much, if any, food-anticipatory activity in their mice. Although Del Río-Martín et al. (2019) attribute an apparent deficit in food anticipation to the *Pitx3*^{ak} gene mutation, their control mice also did not show food anticipation.

Scheduling of food access to the entire dark period would further weigh against emergence of food anticipation. Most studies of food anticipation provide food in the middle of the light period, when activity levels are normally low in control animals, and anticipatory activity can be clearly distinguished from nocturnal activity. In our experiment 2, the mice were fed in the middle of the light period, the amount of food was adjusted to achieve ~10% or greater weight loss, and the feeding schedule was maintained for up to 55 days. With this procedure we observed robust food anticipation in all control and *Pitx3*^{ak} mice, and we did not see evidence that the free-running activity rhythm in the *Pitx3*^{ak} mice was entrained by the feeding schedule, as might be expected if clock gene rhythms in the *Pitx3*^{ak} SCN synchronize to mealtime, as reported by Del Río-Martín et al. (2019).

Del Río-Martín et al. (2019) conclude that failure of the retina to develop and innervate the SCN pacemaker in *Pitx3*^{ak} mice permanently impairs cyclic metabolic homeostasis and entrainment of behavioral rhythms to feeding schedules. This is a provocative idea, a variation of which was suggested independently from work with genetically and neonatally blinded mice (Fernandez et al., 2020). Our analysis of the *Pitx3*^{ak} mouse does not lend support to this model, at least with respect to coordination of behavioral and metabolic rhythms with feeding schedules.

Several lines of evidence point to an important role for dopamine signaling in the dorsal striatum for induction or expression of food-anticipatory circadian activity rhythms, but which and how many of the dopamine neurons are necessary for this rhythm are not known (Assali et al., 2021; Gallardo et al., 2014a; Liu et al., 2012; Michalik et al., 2015; Smit et al., 2013). *Pitx3*^{ak} mice develop only a small fraction of the normal complement of SN dopamine neurons responsible for dopamine signaling in the dorsal striatum, and therefore we were fully expecting to see a significant deficit in food-anticipatory rhythms. Failure to observe a deficit despite a >90% reduction in the number of SN dopamine neurons likely reflects the robust compensatory mechanisms known to be induced in the dorsal striatum in this and other models of chronic dopamine depletion (Hwang et al., 2005; Sagot et al., 2018; Wang and Zhou, 2017). Our results may define a minimum population of SN dopamine neurons sufficient for food entrainment. To test this hypothesis directly, we attempted to delete TH from the Pitx3 lineage but were unable to conduct behavioral experiments using these mice because of early postnatal lethality. Further genetic identification of this population is warranted to fully delineate the role of dopamine signaling in food-entrained metabolic and activity rhythms.

STAR★METHODS

Detailed methods are provided in the online version of this paper and include the following:

- KEY RESOURCES TABLE
- RESOURCE AVAILABILITY
  - Lead contact
  - Materials availability
  - Data and code availability
- EXPERIMENTAL MODEL AND SUBJECT DETAILS
  - Food Intake and Caloric Restriction Conditions
  - Metabolic measurements
  - Measurement of home-cage activity
  - Tissue Histology and Antibody Labeling
- QUANTIFICATION AND STATISTICAL ANALYSIS

SUPPLEMENTAL INFORMATION

Supplemental information can be found online at https://doi.org/10.1016/j.celrep.2021.109865.

ACKNOWLEDGMENTS

This work was supported by a Whitehall Foundation research grant (to A.D.S.) and by the National Institute of General Medical Sciences of the National Institutes of Health (award number SC3GM125570 to A.D.S.). The content is solely the responsibility of the authors and does not necessarily represent the official views of the National Institutes of Health. The funders had no role in study

design, data collection and analysis, decision to publish, or preparation of the manuscript.

AUTHOR CONTRIBUTIONS

Conceptualization, R.E.M. and A.D.S.; methodology, L.L.S., B.W., M.S., R.E.M., and A.D.S.; investigation, L.L.S., B.W., M.S., R.E.M., and A.D.S.; writing – original draft, R.E.M. and A.D.S.; writing – review & editing, L.L.S., B.W., M.S., R.E.M., and A.D.S.; funding acquisition, A.D.S.; resources, B.W., M.S., and A.D.S.; and supervision, A.D.S.

DECLARATION OF INTERESTS

The authors declare no competing interests.

Received: August 25, 2020
Revised: April 6, 2021
Accepted: September 30, 2021
Published: January 11, 2022

REFERENCES

Assali, D.R., Sidikpramana, M., Villa, A.P., Falkenstein, J., and Steele, A.D. (2021). Type 1 dopamine receptor (D1R)-independent circadian food anticipatory activity in mice. PLoS ONE *16*, e0242897.

Damiola, F., Le Minh, N., Preitner, N., Kornmann, B., Fleury-Olela, F., and Schibler, U. (2000). Restricted feeding uncouples circadian oscillators in peripheral tissues from the central pacemaker in the suprachiasmatic nucleus. Genes Dev. *14*, 2950–2961.

Del Río-Martín, A., Pérez-Taboada, I., Fernández-Pérez, A., Moratalla, R., de la Villa, P., and Vallejo, M. (2019). Hypomorphic Expression of Pitx3 Disrupts Circadian Clocks and Prevents Metabolic Entrainment of Energy Expenditure. Cell Rep. *29*, 3678–3692.e4.

Dibner, C., Schibler, U., and Albrecht, U. (2010). The mammalian circadian timing system: organization and coordination of central and peripheral clocks. Annu. Rev. Physiol. *72*, 517–549.

Fernandez, D.C., Komal, R., Langel, J., Ma, J., Duy, P.Q., Penzo, M.A., Zhao, H., and Hattar, S. (2020). Retinal innervation tunes circuits that drive nonphotic entrainment to food. Nature *581*, 194–198.

Fernández-Pérez, A., Sanz-Magro, A., Moratalla, R., and Vallejo, M. (2022). Restricting feeding to the dark phase fails to entrain circadian locomotor activity and energy expenditure oscillations in *Pitx3*-mutant *Aphakia* mice. Cell Rep. *38*, 110241.

Foster, R.G., Hughes, S., and Peirson, S.N. (2020). Circadian Photoentrainment in Mice and Humans. Biology (Basel) *9*, 180.

Gallardo, C.M., Darvas, M., Oviatt, M., Chang, C.H., Michalik, M., Huddy, T.F., Meyer, E.E., Shuster, S.A., Aguayo, A., Hill, E.M., et al. (2014a). Dopamine receptor 1 neurons in the dorsal striatum regulate food anticipatory circadian activity rhythms in mice. eLife *3*, e03781.

Gallardo, C.M., Hsu, C.T., Gunapala, K.M., Parfyonov, M., Chang, C.H., Mistlberger, R.E., and Steele, A.D. (2014b). Behavioral and neural correlates of acute and scheduled hunger in C57BL/6 mice. PLoS ONE *9*, e95990.

Golombek, D.A., and Rosenstein, R.E. (2010). Physiology of circadian entrainment. Physiol. Rev. *90*, 1063–1102.

Honma, K., von Goetz, C., and Aschoff, J. (1983). Effects of restricted daily feeding on freerunning circadian rhythms in rats. Physiol. Behav. *30*, 905–913.

Hood, S., Cassidy, P., Cossette, M.P., Weigl, Y., Verwey, M., Robinson, B., Stewart, J., and Amir, S. (2010). Endogenous dopamine regulates the rhythm of expression of the clock protein PER2 in the rat dorsal striatum via daily activation of D2 dopamine receptors. J. Neurosci. *30*, 14046–14058.

Hwang, D.Y., Fleming, S.M., Ardayfio, P., Moran-Gates, T., Kim, H., Tarazi, F.I., Chesselet, M.F., and Kim, K.S. (2005). 3,4-Dihydroxyphenylalanine reverses the motor deficits in Pitx3-deficient aphakia mice: behavioral characterization of a novel genetic model of Parkinson's disease. J. Neurosci. *25*, 2132–2137.

Lamonerie, T., Tremblay, J.J., Lanctôt, C., Therrien, M., Gauthier, Y., and Drouin, J. (1996). Ptx1, a bicoid-related homeo box transcription factor involved in transcription of the pro-opiomelanocortin gene. Genes Dev. *10*, 1284–1295.

Lebel, M., Gauthier, Y., Moreau, A., and Drouin, J. (2001). Pitx3 activates mouse tyrosine hydroxylase promoter via a high-affinity binding site. J. Neurochem. *77*, 558–567.

LeSauter, J., Balsam, P.D., Simpson, E.H., and Silver, R. (2020). Overexpression of striatal D2 receptors reduces motivation thereby decreasing food anticipatory activity. Eur. J. Neurosci. *51*, 71–81.

Liu, Y.Y., Liu, T.Y., Qu, W.M., Hong, Z.Y., Urade, Y., and Huang, Z.L. (2012). Dopamine is involved in food-anticipatory activity in mice. J. Biol. Rhythms *27*, 398–409.

Michalik, M., Steele, A.D., and Mistlberger, R.E. (2015). A sex difference in circadian food-anticipatory rhythms in mice: Interaction with dopamine D1 receptor knockout. Behav. Neurosci. *129*, 351–360.

Mistlberger, R.E. (2020). Food as circadian time cue for appetitive behavior. F1000Res. *9*, F1000 Faculty Rev-61. https://doi.org/10.12688/f1000research.20829.1.

Nunes, I., Tovmasian, L.T., Silva, R.M., Burke, R.E., and Goff, S.P. (2003). Pitx3 is required for development of substantia nigra dopaminergic neurons. Proc. Natl. Acad. Sci. USA *100*, 4245–4250.

Sagot, B., Li, L., and Zhou, F.M. (2018). Hyperactive Response of Direct Pathway Striatal Projection Neurons to L-dopa and D1 Agonism in Freely Moving Parkinsonian Mice. Front. Neural Circuits *12*, 57.

Schibler, U. (2009). The 2008 Pittendrigh/Aschoff lecture: peripheral phase coordination in the mammalian circadian timing system. J. Biol. Rhythms *24*, 3–15.

Smidt, M.P., and Burbach, J.P. (2007). How to make a mesodiencephalic dopaminergic neuron. Nat. Rev. Neurosci. *8*, 21–32.

Smit, A.N., Patton, D.F., Michalik, M., Opiol, H., and Mistlberger, R.E. (2013). Dopaminergic regulation of circadian food anticipatory activity rhythms in the rat. PLoS ONE *8*, e82381.

Stephan, F.K., and Becker, G. (1989). Entrainment of anticipatory activity to various durations of food access. Physiol. Behav. *46*, 731–741.

Wang, Y., and Zhou, F.M. (2017). Striatal But Not Extrastriatal Dopamine Receptors Are Critical to Dopaminergic Motor Stimulation. Front. Pharmacol. *8*, 935.

STAR★METHODS

KEY RESOURCES TABLE

REAGENT or RESOURCE	SOURCE	IDENTIFIER
Antibodies		
tyrosine hydroxylase	Aves	TYH
Goat anti-chicken, AlexaFluor 647	ThermoFisher	A-21449
Chemicals, peptides, and recombinant proteins		
Phosphate buffered saline	VWR	97062-730
DAPI	Thermofisher	D-1306
Paraformaldehyde	Sigma	P6148
Experimental models: Organisms/strains		
Pitx3^{ak} mice	The Jackson Laboratory	000942
Oligonucleotides		
"OR-72F" CTCTCCAGCCTC CCTCAAATACT	IDT	n/a
"OR-75R" TCGGATTTGGCTTCTGATGGTTTT	IDT	n/a
"Pitx3-set3-F" ATTAGAGGTCGTTCAGGATG	IDT	n/a
"Pitx3-set3-R" TAATTGAGGCCTTGGGCTCT	IDT	n/a
Software and algorithms		
Graphpad Prism 6	Graphpad	https://www.graphpad.com
Oxymax	Columbus Instruments	https://www.colinst.com/products/clams-comprehensive-lab-animal-monitoring-system
Clocklab	Actimetrics, IL	Clocklab software
Other		
PicoVac rodent diet	Labdiet	5061
Rodent chow	Teklad	2018
Metabolic cages and equipment	TSE systems	TSE phenomaster
Activity cages	Columbus Instruments	CLAMS
Whole Body Magnetic Resonance Analyzer System	EchoMRI	EchoMRI-700

RESOURCE AVAILABILITY

Lead contact

Further information and requests for resources and reagents should be directed to and will be fulfilled by the lead contact, Andrew Steele (adsteele@cpp.edu), and the additional corresponding author, Ralph Mistlberger (mistlber@sfu.ca).

Materials availability

This study did not generate new unique reagents.

Data and code availability

Datasets available upon request from the lead contacts.

EXPERIMENTAL MODEL AND SUBJECT DETAILS

Pitx3^{ak} mice (strain 000942) were obtained from the Jackson Laboratory's cryorepository. The aphakia allele arose spontaneously in a 129S1/Sv-p+ Tyr+ KitlSl-J/J strain that was subsequently backcrossed to C57BLKS/J and then to C57BL/6J using homozygous

males at generation N5F39 or N5F40 bred to C57BL/6J females. All mice used for experiments were derived by intercrossing heterozygous mutants to produce age- and sex-matched littermate controls.

All experiments involving the use of animals were approved by the Institutional Animal Care and Use Committee of California State Polytechnic University, Pomona, CA under protocols 16.029 and 17.003.

Genomic DNA samples were isolated from proteinase K-digested tail tissue using an isopropanol precipitation. Pitx alleles were amplified using the following primers: 'OR-72F' CTCTCCAGCCTCCCTCAAATACT, 'OR-75R' TCGGATTTGGCTTCTGATGGTTTT, 'Pitx3-set3-F'ATTAGAGGTCGTTCAGGATG, and 'Pitx3-set3-R' TAATTGAGGCCTTGGGCTCT. PCR cycling conditions were as follows: 95°C for 5 minutes, 35 cycles at 94°C for 30 s, 58°C for 30 s, and 72°C for 1.5 minutes followed by 1 cycle at 72°C for 10 minutes. Results were visualized on a 2% agarose gel.

All mice were maintained on a 12:12 light:dark cycle (70 lux fluorescent with lights on, 0 lux with lights off) throughout all experiments. All mice were single housed in static microisolator cages containing sani-chip bedding (Envigo, 7090) and a cotton nestlet. Room temperature was maintained at 22-24°C with humidity at 20%–45%. Light levels were 168 lux at the Cal Poly Pomona facility and 82 lux at the USC/CHLA Metabolic Core facility.

Food Intake and Caloric Restriction Conditions

In Experiment 1 (metabolism study), the mice were fed LabDiet #5061 chow ad-libitum for 3 days to quantify average daily intake. During restricted feeding, the mice were provided 80% of their average daily caloric intake for 28 days, with food delivered in the middle of the light period (6h after light onset). In Experiment 2 (locomotor activity study), the mice were fed Teklad 2018 (18% protein) chow. Caloric restriction was maintained at 80% in the *Pitx3*^{ak} mice and reduced to 60% in the control mice, to achieve equivalent body weight reductions. Mice on the 80% schedule were weighed weekly, while mice on 60% schedule were weighed three times per week.

Metabolic measurements

In Experiment 1, control and *Pitx3*^{ak} mice (n = 6 males and females per group) were studied at Children's Hospital Los Angeles/USC for body composition, metabolic, and behavioral entrainment to scheduled feeding. The EchoMRI-700 Whole Body Magnetic Resonance Analyzer System was utilized for measurements of body fat, lean mass, body fluids and total body water. The TSE LabMaster/PhenoMaster Metabolic Phenotyping System was used to collect data on energy expenditure by indirect calorimetry, feeding behavior and physical activity. Parameters were measured for 7 consecutive days (3 days on *ad libitum*, 4 days on caloric restriction), then again for 3 additional days on days 26 to 28 of 80% restriction. Circadian timing of metabolic variables measured in Experiment 1 was quantified by calculating the acrophase of a sine wave fit to each day of recording, using Clocklab software (Actimetrics, IL).

Measurement of home-cage activity

In Experiment 2, mice were fed Harlan Teklad 2018 chow and their activity was measured using a modified Comprehensive Lab Animal Monitoring System from Columbus Instruments (Columbus, OH), which monitored activity continuously with measurements collected in 5 minute bins based on the number of infra-red beam breaks across x-,y-, and z-axes. Activity was visualized using ClockLab software (Actimetrics, Il) and GraphPad Prism 8 (GraphPad Software, San Diego CA). Circadian periodicity in the activity data from Experiment 2 was quantified using the F-periodogram as implemented in Clocklab.

Tissue Histology and Antibody Labeling

Transcardiac perfusion was performed by injecting 5-10 mL of phosphate buffer into the left ventricle followed by 5 mL of 4% PFA (Sigma), both made fresh prior to perfusion. Whole brain tissue was removed and stored in 4% PFA at −4C for 24 hours, then placed in 0.1M PBS. 50-micron coronal and sagittal sections were obtained using a Leica VT1000S Vibratome (Leica Biosystems, Buffalo Grove, IL) and stored in 0.1M PBS at −4°C.

Tissue samples were placed in glass well plates in 0.1M PBS for 1 minute, then permeabilized by incubating in PBST (0.5% Triton X-100 in PBS) for 10 minutes. Samples were then blocked in goat serum for 10 minutes. Tissue samples were diluted in a tyrosine hydroxylase primary antibody (Aves Lab, Tigard, OR; Catalog #TYH) diluted in goat serum overnight then washed three times in PBS for 5 minutes each. Tissue was submerged in a 1:500 dilution of secondary antibody (Goat anti-chicken, AlexaFluor 647, ThermoFisher, Catalog #A-21449) to PBS for 1 hour. The tissue samples were washed in PBS two times for 5 minutes each then added to a DAPI solution for 5 minutes. Tissue samples were washed again for 5 minutes in PBS before being mounted.

Imaging was performed using a Nikon C2 Confocal scope with a standard detector system and Nikon Elements Software.

QUANTIFICATION AND STATISTICAL ANALYSIS

Statistical significance of group differences was evaluated by ANOVA or t tests conducted using GraphPad Prism 8, as described in the main text. Graphs were prepared using GraphPad Prism and figure layouts were created using Adobe Illustrator.

Cell Reports, Volume *38*

Supplemental information

Mice hypomorphic for *Pitx3* show robust entrainment of circadian behavioral and metabolic rhythms to scheduled feeding

Lori L. Scarpa, Brad Wanken, Marten Smidt, Ralph E. Mistlberger, and Andrew D. Steele

Figure S1. Body mass, body composition, daily energy expenditure (EE), daily activity, and daily food intake in control (CTL) and *Pitx3*^{ak} mice in metabolic cages with food available ad-libitum (Experiment 1). Blue bars = males, red bars = females. Results of 2-way (Pitx3 genotype x sex) ANOVA are provided. Related to Figure 1.

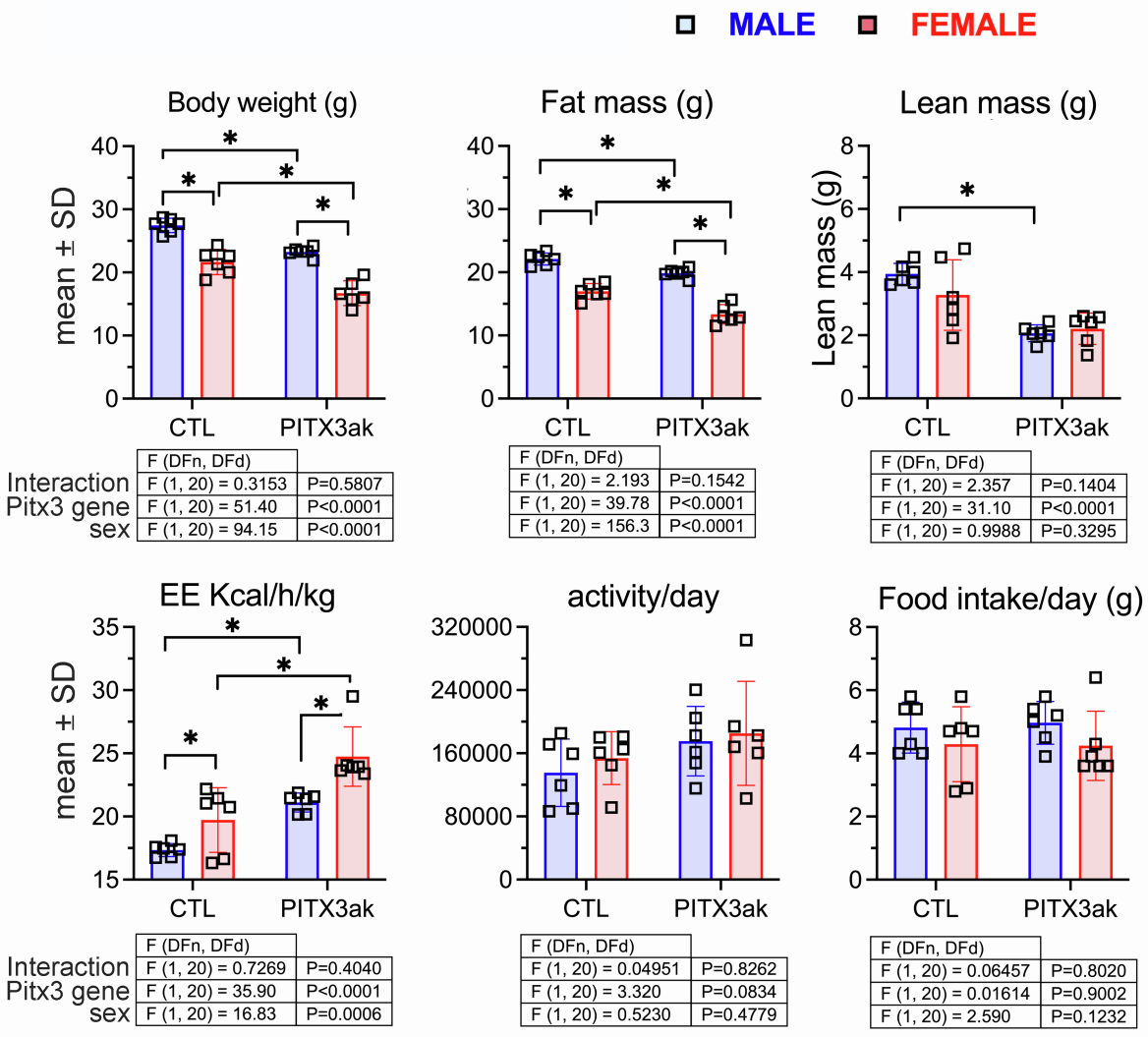

Figure S2. Energy expenditure per hour in male (blue) and female (red) control (CTL) and *Pitx3^{ak}* mice with food available ad-libitum in metabolic cages for 72 h (Experiment 1). The top row shows group means for males (left panel) and females (right panel), after aligning the *Pitx3^{ak}* mice with each other, and then aligning the group waveform with the control group waveform. The lower 6 rows show energy expenditure of individual mice before and after smoothing. Related to Figure 2.

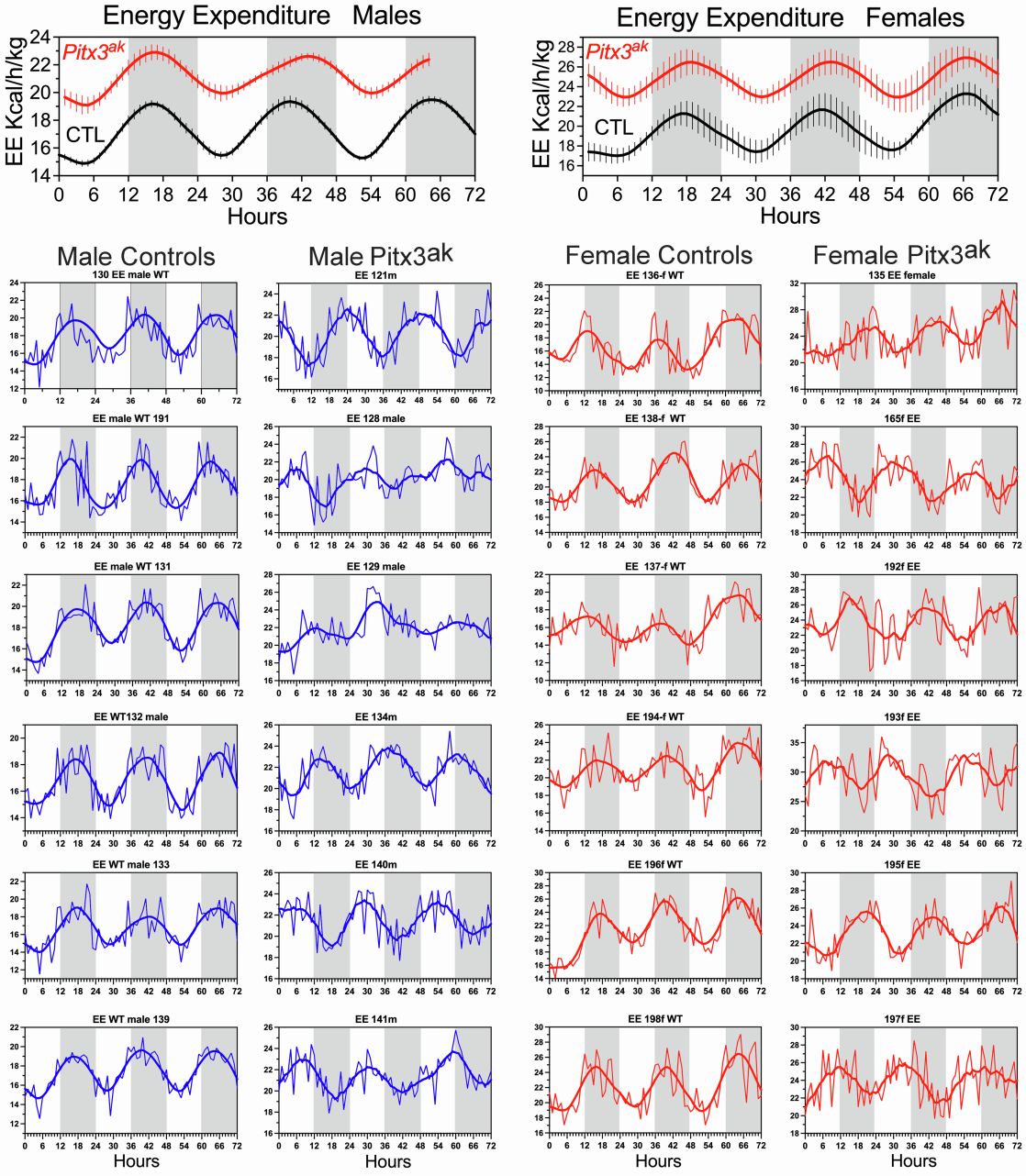

Figure S3. Food intake and weight change during restricted feeding (Experiment 1). (A-D) Hourly food intake of individual male (left column) and female (right column) control (CTL, black lines) and *Pitx3*^{ak} mice (red lines) averaged over the last 3 days of restricted feeding (days 26-28). (E,F). Group averages. (G,H) Cumulative food intake. (I,J) Body weight, lean mass and fat mass, on the last day of restricted feeding expressed as a percentage of weights recorded on the last day of ad-libitum food access. Related to Figure 3

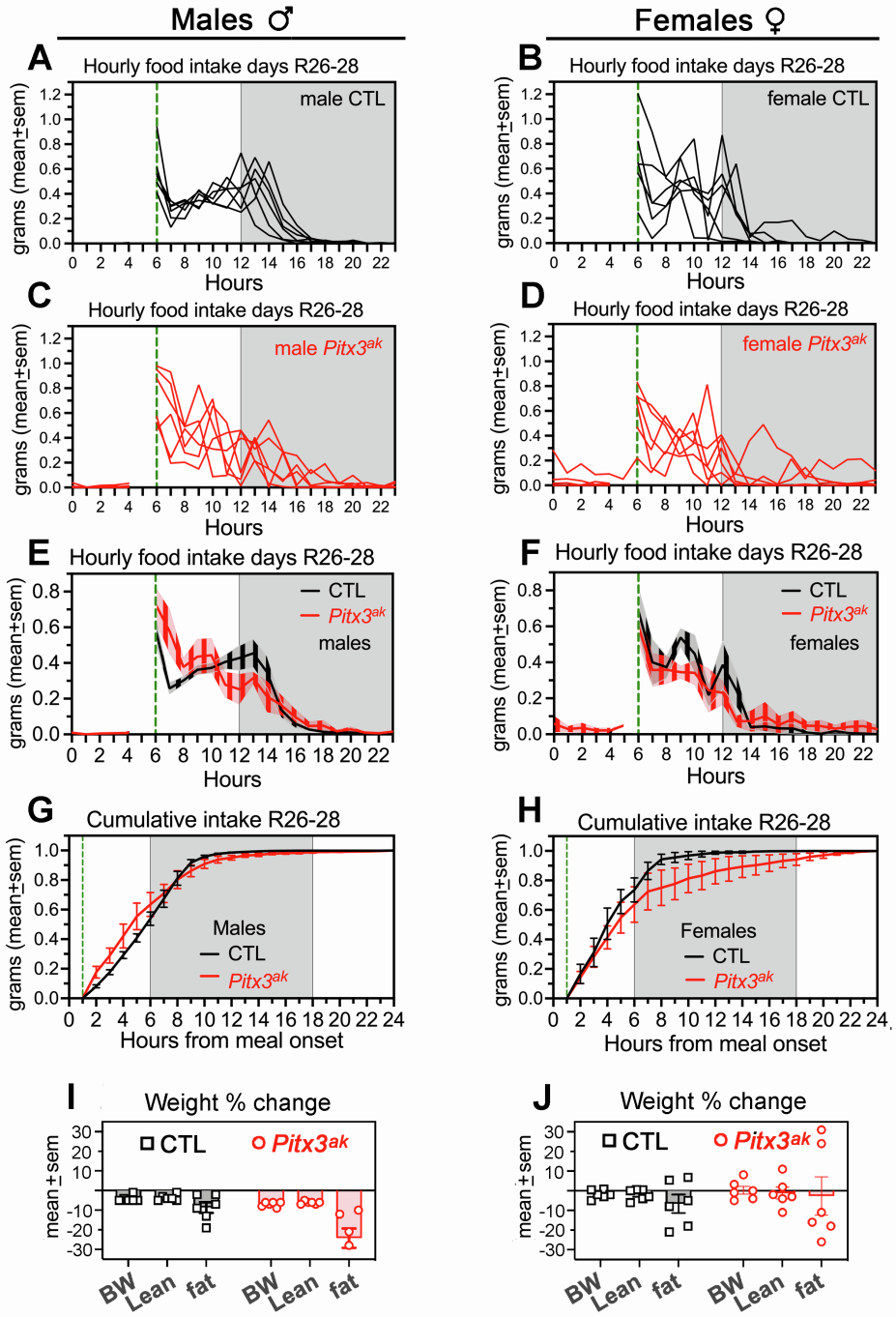

Figure S4. Circadian Activity Rhythms in *Pitx3ak* and control mice with food available ad-libitum (Experiment 2). Actograms of locomotor activity prior to restricted feeding in (A) 8 female control mice (CTL, c1-8), and (B) 7 female *Pitx3^{ak}* mice (ak1-7). Activity data are plotted in 10 min times plotted from left to right within a day, and consecutive days are aligned both vertically and horizontally (the graphs are 'double-plotted, so that each line represents 48h). Grey shading denotes lights-off. The time scale for each *Pitx3ak* mouse was set to the period (*greek letter tau*) of the free-running rhythm, as determined by F-periodogram analysis. (C) Group mean (+SEM) waveform of locomotor activity from the 8 CTL mice (black curve) averaged across 24h days, and from the 7 *Pitx3ak* mice (red curve) averaged modulo-*tau* for each mouse, and then averaged across the group after aligning the individual educed waveforms by the first peak of activity. (D) Group mean (±SD) of activity counts per 24h or circadian cycle. (E) The duration of the daily active period (*greek letter alpha*). (F) The ratio of activity in *alpha* to activity in the rest phase (*greek letter rho*) (G) The relative amplitude (RA) of the activity rhythm. (H) The intradaily variability of the rest-activity rhythm. *p<.05 by ANOVA (Sidak's post hoc test). (I) Educed waveforms of locomotor activity for each *Pitx3^{ak}* mouse. The time series were folded modulo tau to create the waveform for each mouse (left column) which when averaged across mice (K) yielded an arrhythmic group waveform. (J) Educed waveforms aligned by the first peak of activity, yielding a robust group average waveform (L, and C). Related to Figure 4.

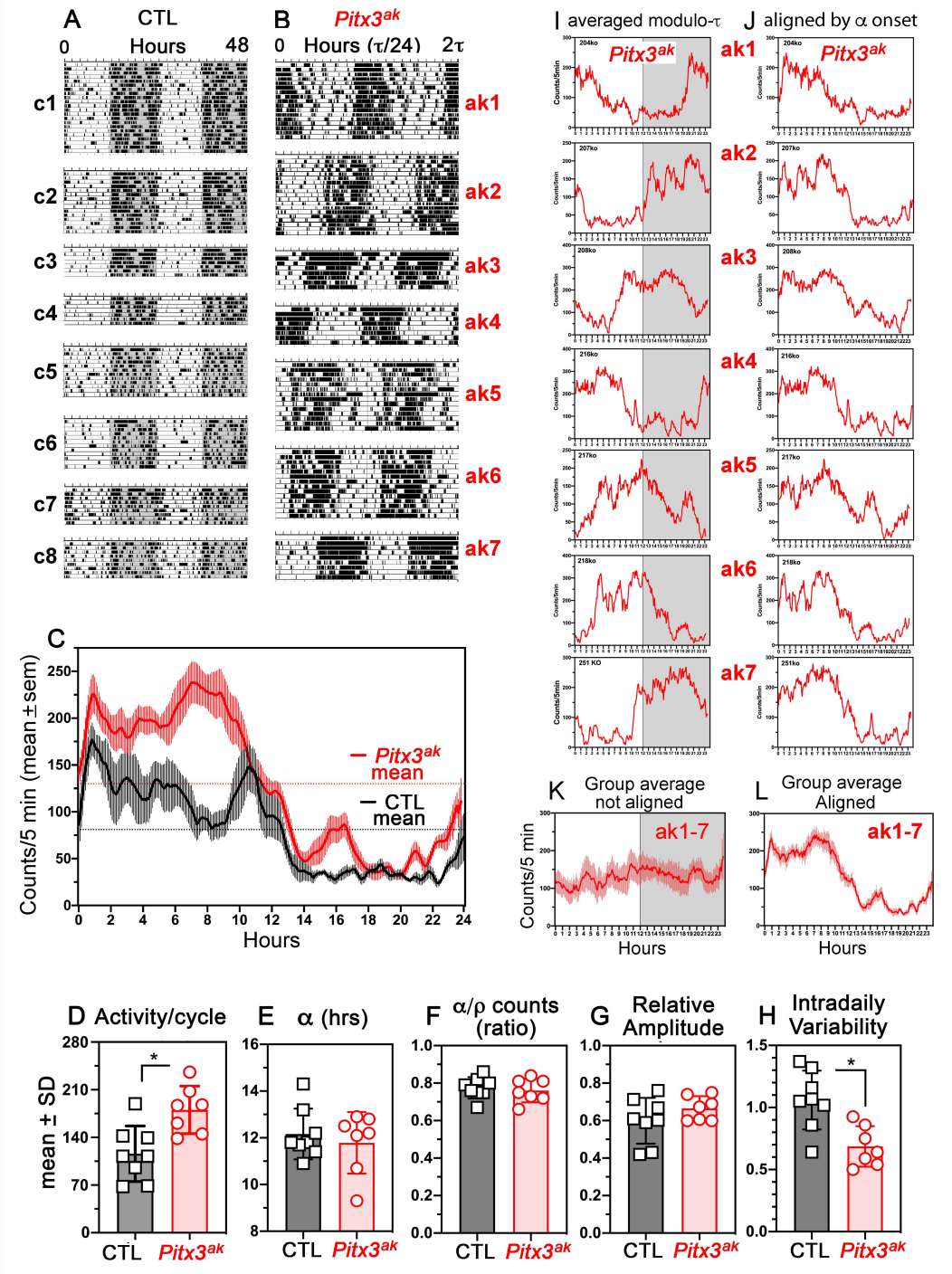

Figure S5. Tyrosine Hydroxylase Antibody Labeling. (A) sagittal section of control brain and (B) Pitx3^{ak} substantially less innervation of the striatum and nucleus accumbens in Pitx3ak sections. We stained consecutive coronal sections of the midbrain with TH antibody to visualize the dopamine neurons in the SN and VTA. Control midbrains showed numerous dopamine neurons in the VTA and SN (C) while the Pitx3ak midbrain showed very little TH staining in the SN but ample staining in the VTA. Related to Figure 4.